NRIAG Journal of Astronomy and Geophysics (2015) **4**, 266–282

National Research Institute of Astronomy and Geophysics

NRIAG Journal of Astronomy and Geophysics

www.elsevier.com/locate/nrjag

Application of gamma ray spectrometric measurements and VLF-EM data for tracing vein type uranium mineralization, El-Sela area, South Eastern Desert, Egypt

Ibrahim Gaafar

Nuclear Materials Authority, Egypt

Received 25 March 2015; revised 27 September 2015; accepted 3 October 2015
Available online 21 October 2015

KEYWORDS

Gamma ray;
El Sela shear zone;
VLF-EM data;
Conductivity

Abstract This study is an attempt to use the gamma ray spectrometric measurements and VLF-EM data to identify the subsurface structure and map uranium mineralization along El Sela shear zone, South Eastern Desert of Egypt. Many injections more or less mineralized with uranium and associated with alteration processes were recorded in El Sela shear zone. As results from previous works, the emplacement of these injections is structurally controlled and well defined by large shear zones striking in an ENE–WSW direction and crosscut by NW–SE to NNW–SSE fault sets. VLF method has been applied to map the structure and the presence of radioactive minerals that have been delineated by the detection of high uranium mineralization. The electromagnetic survey was carried out to detect the presence of shallow and deep conductive zones that cross the granites along ENE–WSW fracturing directions and to map its spatial distribution. The survey comprised seventy N–S spectrometry and VLF-EM profiles with 20 m separation. The resulted data were displayed as composite maps for K, eU and eTh as well as VLF-Fraser map. Twelve profiles with 100 m separation were selected for detailed description. The VLF-EM data were interpreted qualitatively as well as quantitatively using the Fraser and the Karous–Hjelt filters. Fraser filtered data and relative current density pseudo-sections indicate the presence of shallow and deep conductive zones that cross the granites along ENE–WSW shearing directions. High uranium concentrations found just above the higher apparent current-density zones that coincide with El-Sela shear zone indicate a positive relation between conductivity and uranium minerals occurrence. This enables to infer that the

E-mail address: Ibrahim.gaafar@hotmail.com

Peer review under responsibility of National Research Institute of Astronomy and Geophysics.

ELSEVIER Production and hosting by Elsevier

http://dx.doi.org/10.1016/j.nrjag.2015.10.001

anomalies detected by VLF-EM data are due to the highly conductive shear zone enriched with uranium mineralization extending for more than 80 m.

1. Introduction

Radioactive minerals occur naturally in the geological environment associated with geological features such as unconformity contact, veins, shear zones, and so forth (Tuncer et al., 2006).

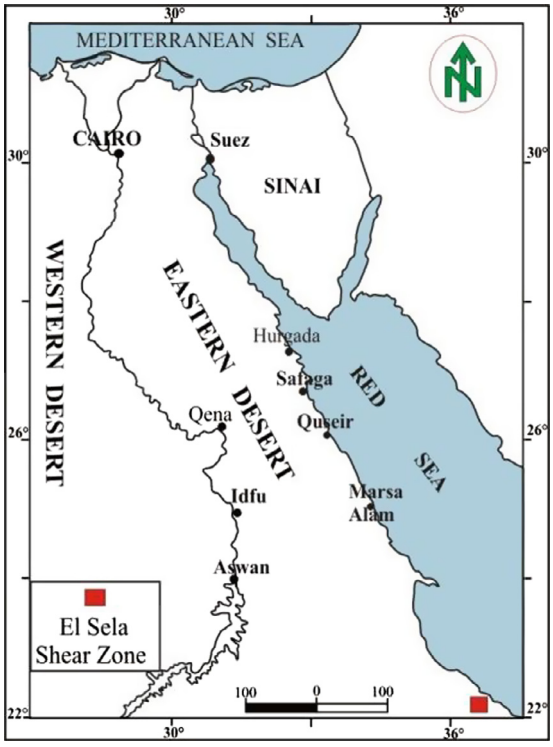

Figure 1 Location map of El-Sela shear zone, South Eastern Desert (S E D), Egypt.

The nature of mineralization varies from hydrothermal vein type, strata bound deposit, disseminated type, and brecciated complex in the form of vertical, dipping, and horizontal sheet type structures. This is dependent primarily on the prevailing geological environment and the valence state of uranium, respectively. Such shallow subsurface structures can be best delineated by very low frequency electromagnetic method due to its advantage in detecting conducting structures. Uranium, being a metal, is highly conducting and, therefore, its presence in the subsurface rocks provides an excellent conductivity contrast between its deposit and the neighbouring formations (Legault et al., 2008; Nimeck and Koch, 2008). Moreover, to prove the presence of radioactive mineralization, radiometric survey is an essential aspect which can differentiate, with a better resolution, between a probable mineralization and that of an economic prospect. Their occurrences in outcrop enhance the background radiation of the area.

Gamma-ray maps reflect the geochemical variations of K, U and Th in the upper 30 cm of the earth's surface. This thin layer is subject to weathering which leads to the loss U and Th concentrations, while K may increase in altered rocks. Th may show increase or decrease during hydrothermal alteration. Detailed interpretation of gamma-ray survey requires the delineation of major geological units and examination of subtle variations with the aid of other data (Charbonneau and Ford, 1979).

Very low frequency-EM method is a semi-passive electromagnetic induction method which utilizes distant high power vertical transmitters as a source for the primary field. These transmitters are meant for long distance marine communications and situated on the coastal areas worldwide. They operate in the lower band (15–30 kHz) of communication frequency. These signals travel a long distance and can be utilized for geophysical measurements several thousand km away from transmitters. Since the primary field is horizontal, VLF

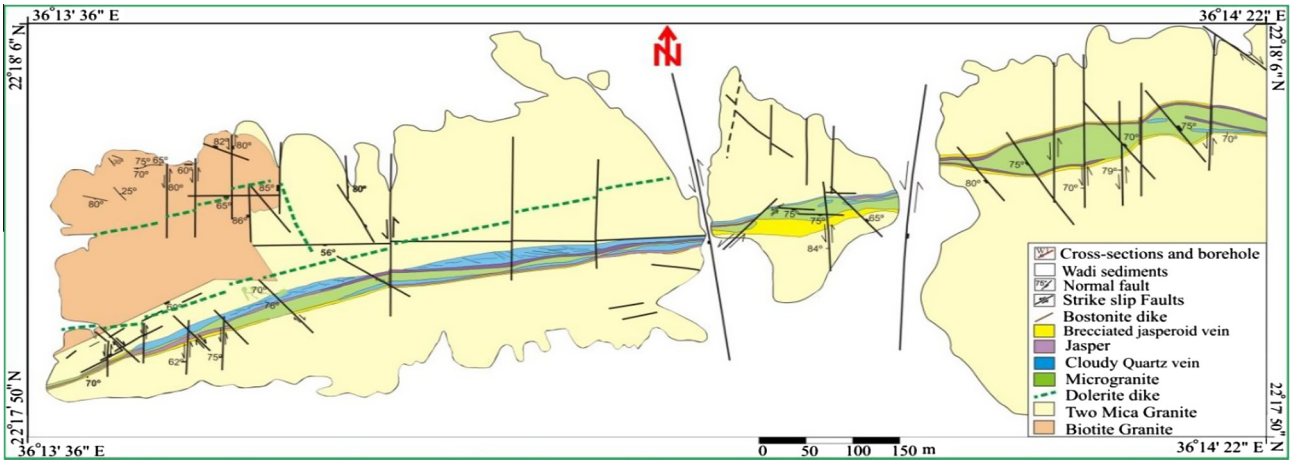

Figure 2 Geologic Map of El-Sela Shear Zone, S E D, Egypt (after Gaafar et al., 2006).

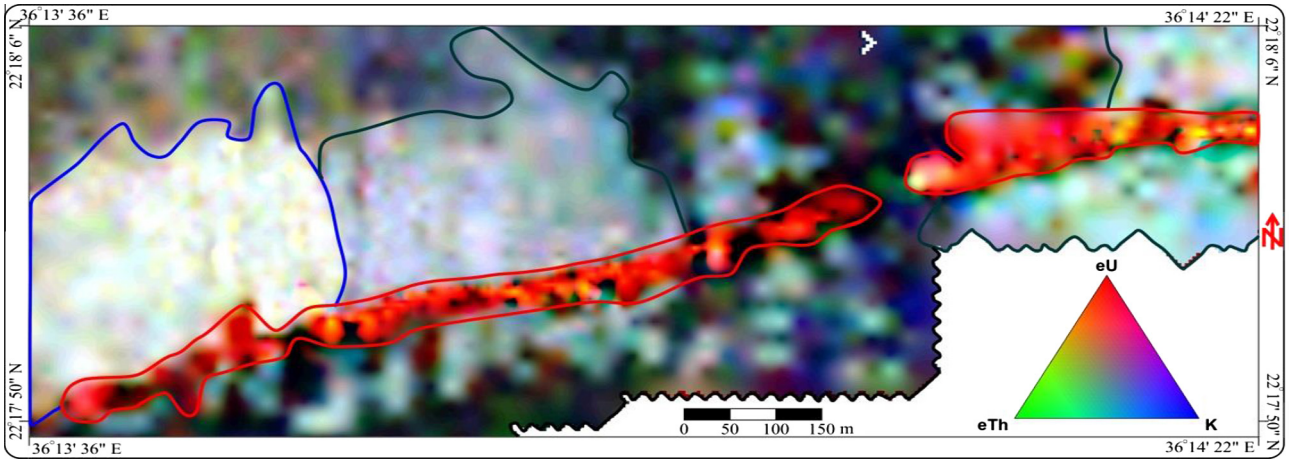

Figure 3 Composite image map (K, eU and eTh) of El-Sela shear zone area.

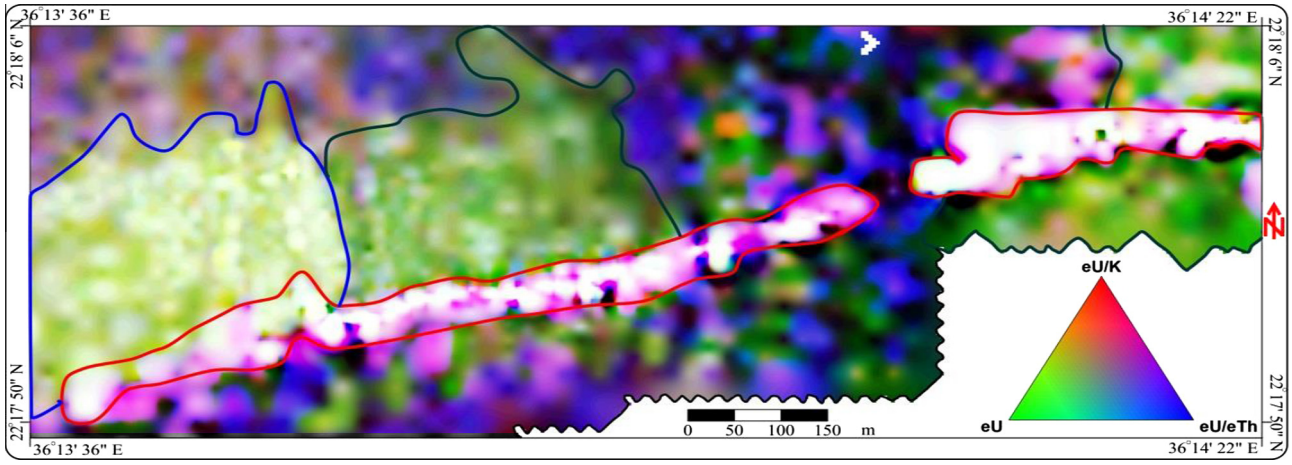

Figure 4 Composite image map (eU, eU/K, and eU/eTh) of El-Sela shear zone area.

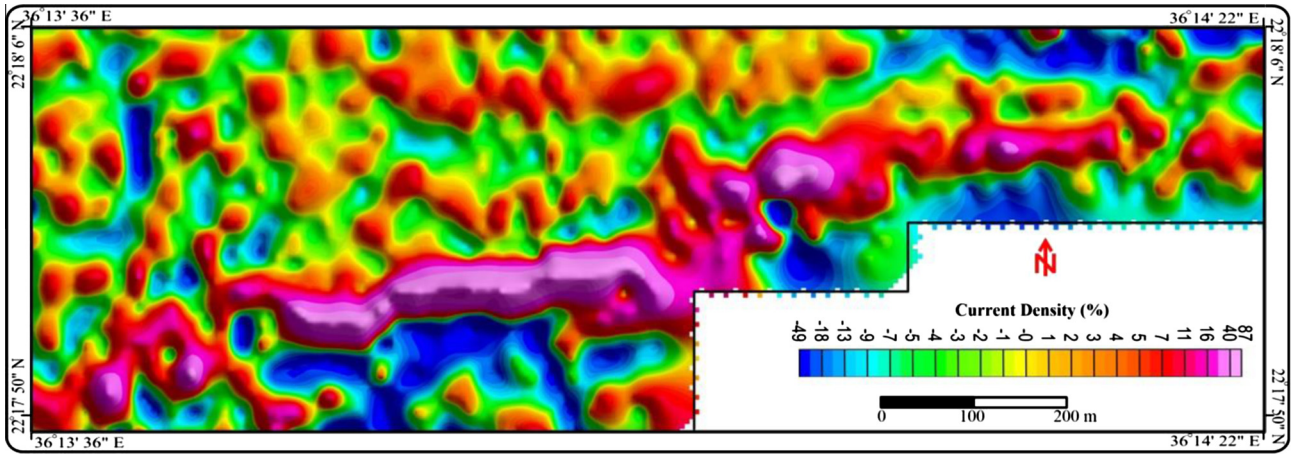

Figure 5 VLF Fraser filter (F = 17.1 kHz) image map for the El-Sela Shear Zone area.

method is ideal for the investigation of vertical and dipping conducting structures in the subsurface. Because of the easy operation of the instrument, speed of field survey, and low operation cost, this method is very suitable for rapid preliminary surveys and has been widely used in many geophysical studies since the 1960s (McNeill and Labson, 1991; Tabbagh et al., 1991; Benson et al., 1997; and Sharma and Baranwal, 2005).

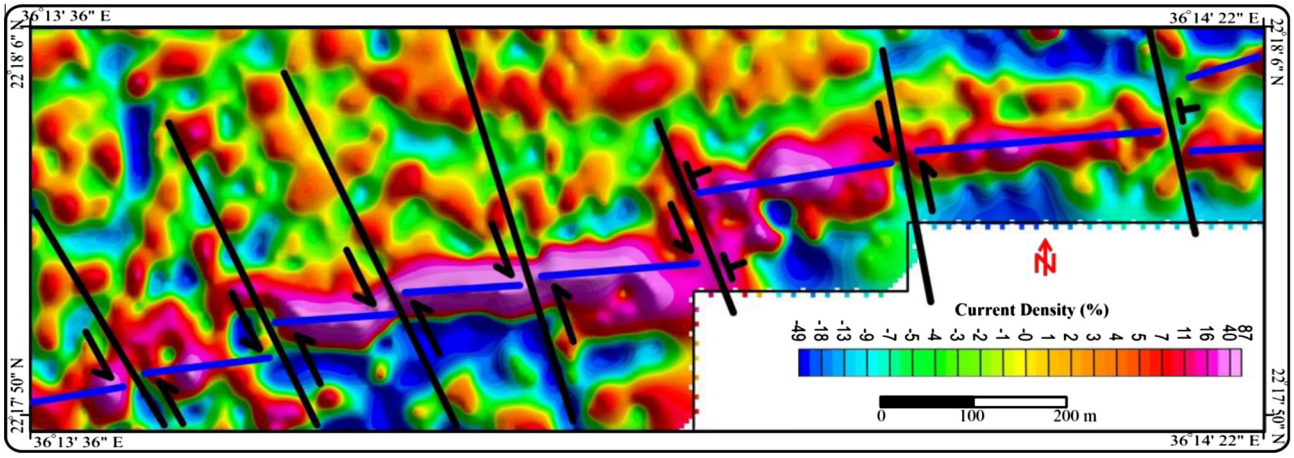

Figure 6 Structural lineaments as deduced from VLF Fraser filter for the El-Sela Shear Zone.

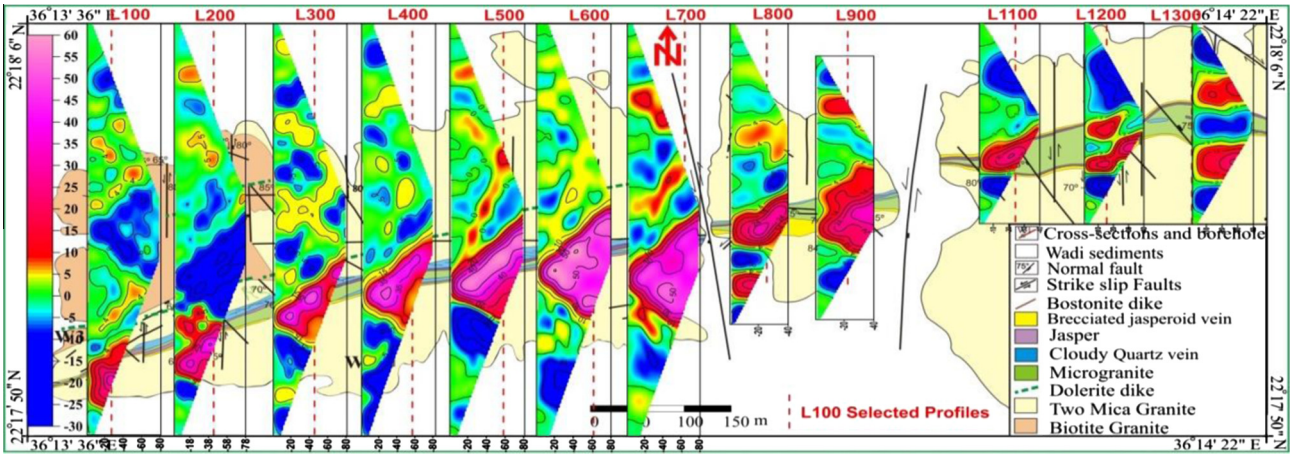

Figure 7 VLF pseudo-sections superimposed on the geologic map of El-Sela shear zone.

During the last decades, VLF surveying has been employed world-wide to identify conducting features in mineral exploration, geological, engineering and environmental problems (Smith et al., 2001; Becken and Pedersen, 2003). The suitability of VLF ground surveys in the investigation of shallow two-dimensional structures is confronted with the practical example of an asymmetrical vertical dike resulting from a strike-slip fault. Modelling of the survey results is very successful and yields good confirmation of the polar behaviour. VLF ground surveys thus provide a quick and powerful tool for the study of geological accidents within about 100 m of the surface (Fischer et al., 1983).

High magnetic anomaly and subsurface signature of uranium from borehole confirm the association of U-minerals with the magnetized minerals El-Sela Shear zone (Gaafar et al., 2006 and Gaafar et al., 2014). Considering these findings, our aim of the survey was to demarcate the actual structure of the uranium deposit body and to trace its possible extension along the shear zone. To achieve this goal, an integrated approach was applied, where very low frequency (VLF) electromagnetic and radiometric surveys were used together. Since the depth of investigation for VLF method depends on skin depth and the radiometric method depends on the lithology of the area as well as on their radioelement contents, these measurements will throw some light in better correlation of uranium mineralization with the prevailing structure.

2. Geology

El Sela area is located in the southern Eastern Desert of Egypt, between Latitudes 22°17′50″N and 22°18′6″N and Longitudes 36°13′36′E and 36°14′22″E, at a distance of about 30 km southwest of Abu-Ramad city (Fig. 1).

The detailed geological and structural studies show that El-Sela area is affected by several successive tectonic events. These events are reflected by high fracture intensity and consequently intense weathering activity. The studied granite is affected by ENE–WSW shear zone dipping 50–70° to the south (Fig. 2). It extends to about 1400 m length with thickness ranging between 2 m and 40 m. The ENE–WSW compression resulted in the NNW–SSE opening due to the permuted NNW–SSE tension and this system was reactivated several times.

During the first reactivation, the ENE–WSW shear plane was injected by white massive quartz rarely containing

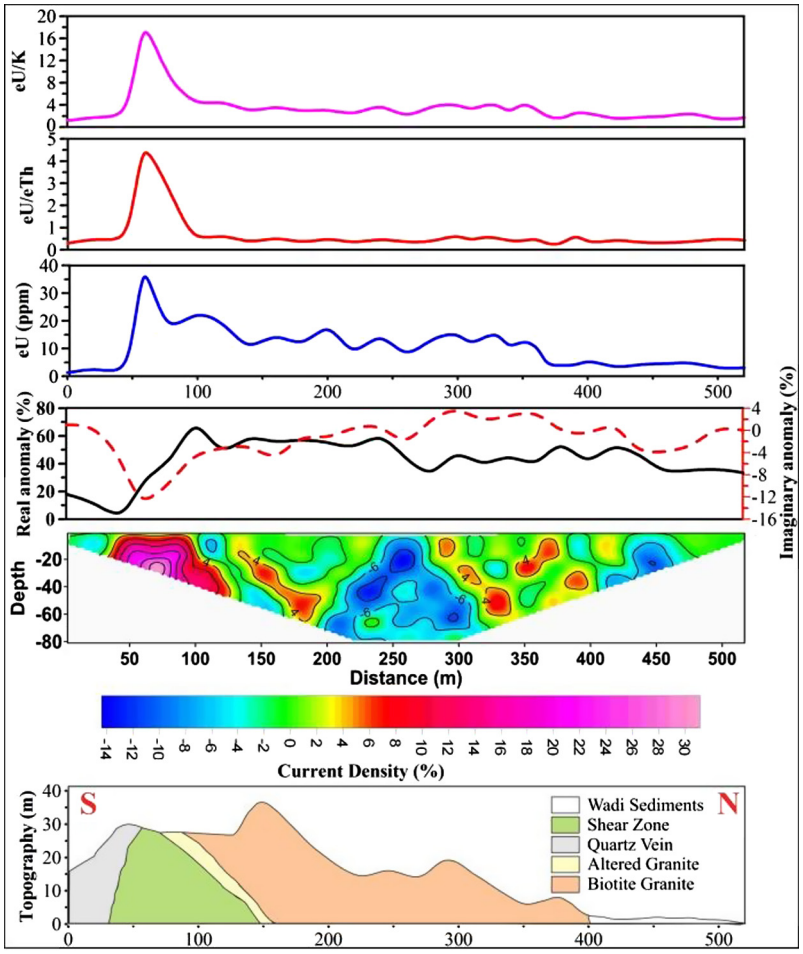

Figure 8 L100, VLF pseudo-sections, eU, eU/eTh, eU/K profiles and interpreted models of El-Sela Shear zone.

amazonite and sulfide crystals as cloudy patches. During the second activation the plane was injected by 1–4 m thick of micro-granite very rich in sulfides. During the third reactivation, the shear zone was injected by highly radioactive beige to pink jasper with a thickness varying from 20 to 40 cm. The fourth reactivation was contemporaneous with discontinuously exposed lamprophyre dyke of thicknesses varying from 20 cm to 3 m. It is mainly composed of large monoclinic crystals of K-feldspar embedded in a fine basic amygdaloidal groundmass rich with calcite. It has high U-content (> 40 ppmeU) many times greater than the granite, so it is considered as uraniferous lamprophyre (Gaafar, 2012).

All the previous injections may eventually have played an important role as uranium, heat, CO_2 and fluids source which may have led to U-mobilization and also its possible trapping along the structure. Most of the feldspar crystals of the lamprophyre have disappeared leaving their boxworks sometimes filled with secondary uranium minerals. All the previous types of injections were hydrothermally altered, brecciated and cemented by the white silica injections that are contemporaneous. Hematitization (red staining) is observed mainly near the bostonite dikes. Episyenitization has been discovered only in the vicinity of the contacts between the two granitic intrusions and generally superimposed by K-metasomatism associated with traces of violet fluorite (Ali, 2011). The highest radioactive anomalies rich with visible uranophane and anthozonite are incorporated with silicified argillic clayey matrix of the altered micro-granite and lamprophyre dykes within the shear zone. The uranium contents attain values up to 3000 ppmeU with relatively high thorium content, which may suggest adding new radioactive elements during the different injections (Gaafar, 2012).

3. Spectrometric composite images

Single channels K, eU and eTh may be significantly affected by these environmental parameters. Reducing the effects can be achieved through simple ratios of natural radioelements. K, eU and eTh ratios calculated from airborne and ground gamma ray spectrometric measurements are used for eliminating the geometry and overburden effects.

Composite images provide a simultaneous display of up to three parameters on one image and facilitate the correlation and delineation of areas based on subtle differences in numerical values. The following combinations are developed by United States Geological Survey (USGS) (Duval, 1983): 1. The radioelement composite image combines the data of K (in blue), eTh (in green), and eU (in red), and 2. The uranium

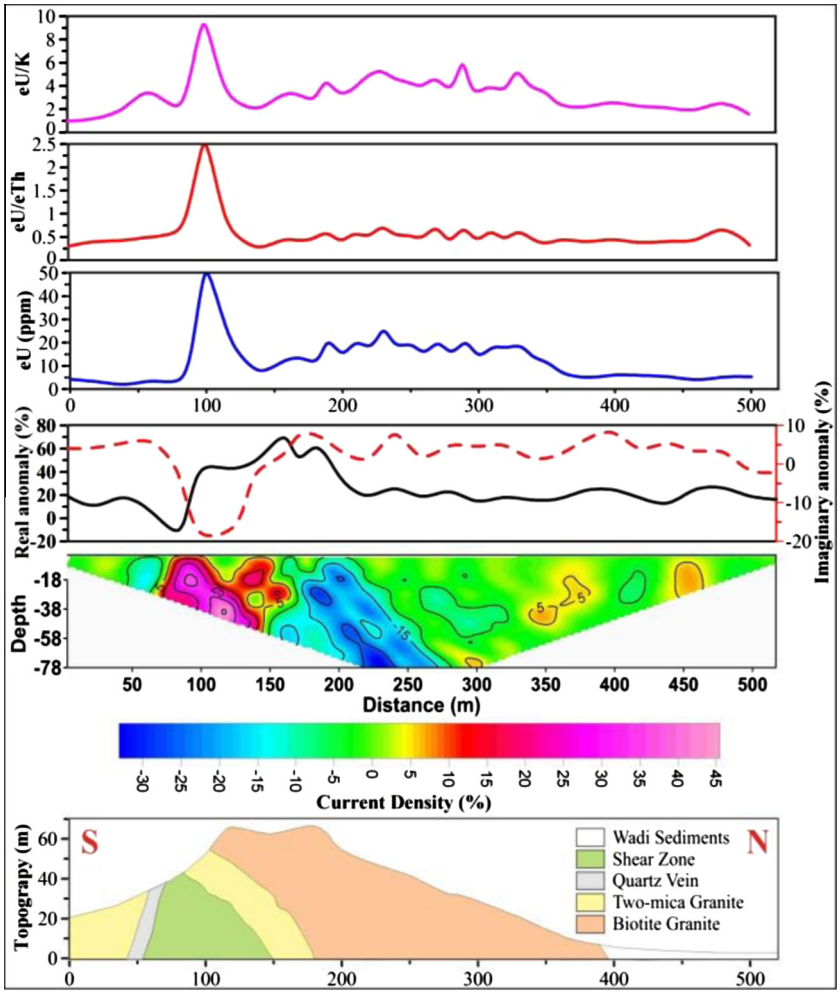

Figure 9 L200, VLF pseudo-sections, eU, eU/eTh, eU/K profiles and interpreted models of El-Sela Shear zone.

composite image combines the data of eU (in green) with the ratios eU/eTh (in blue) and eU/K (in red).

Obviously, there is a good correlation between the geological map and composite image maps of radioactive elements (Figs. 3 and 4). Biotite granite in the western side of the studied area is characterized by an increase of the radioactivity content of the three radioactive elements, so it appears nearly white in color. Meanwhile, the radioactivity contents of the three elements decrease gradually eastwards to the two-mica granite, which is characterized by blue–green color as a result of the predominance of K and eTh. The two-mica granite at the eastern part is slightly high in its radioactivity content discriminated with greenish blue colour due to their relatively high eTh and K contents. Radioactivity content decreases strongly in the low-land younger granite. Wadi sediments as well as quartz veins appear as a mix of dark blue and green black colors, which reflects the level of background radiation for the three radioactive elements in the study area. The most significant highest level of uranium without presence of potassium or thorium is associated with the ENE–WSW shear zone, which takes a distinguished linear anomaly of dark red color. Equivalent uranium contents attain values up to 3000 ppmeU with relatively low eTh and potassium contents which indicates the high U-potentialities of the Sela shear zone. This high U-potentiality is typically associated with the alteration of the sheared rocks, which are associated with uranium mineralization.

Uranium composite image (Fig. 4) shows a very high anomaly that is distinguished by white color due to the simultaneous increase of the three parameters. This anomaly is best developed along the central parts of the study area; where the uranium-bearing shear zone is elongated from the southwest to the northeast (Fig. 4). These uranium anomalies are due to uranium remobilization along the faulted zones. The biotite granites are well discriminated from the two-mica granites by their relatively high content of eU and both of eU/K and eU/eTh so that it is represented by whitish green color. These correlations relate to differentiation trends in the biotite-granitic rocks with relatively high eU/eTh ratio. In the mean time the two-mica granite is characterized by moderate eU content compared with low values of both ratios of eU/eTh and eU/K, so it appears with pale green color. The two-mica granite in the eastern part of the studied area shows predominance of green color, which means that they contain relatively high concentrations of uranium, but they contain low values of eU/eTh and eU/K, and this reduces its importance as a source

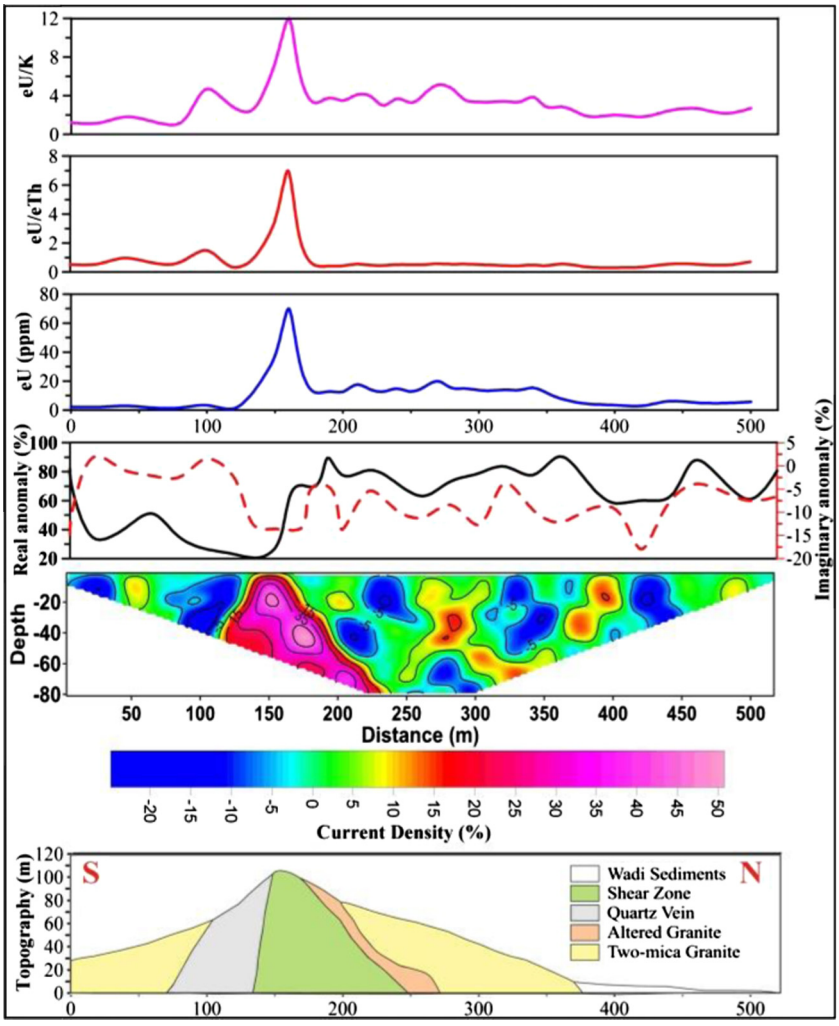

Figure 10 L300, VLF pseudo-sections, eU, eU/eTh, eU/K profiles and interpreted models of El-Sela Shear zone.

of uranium. The wadi sediments and low land granites that are mostly covered with quartz dump do not represent any significant radioactivity increases, and blue color is predominant than green and red which refers to its relatively high eU/eTh ratio.

4. Very low frequency electromagnetic survey

The ENVI VLF instrument was used to collect the VLF measurements for the present study. This instrument measures the component ratio of the vertical of the magnetic field (H_z) which depends on the geological subsurface. The strike of the formation around El-Sela shear zone is approximately in the E–W direction; hence, the transmitter in E–W direction with frequency of 17.1 kHz was selected for E-polarization measurements. VLF surveys were performed along seventy profiles oriented in N–S direction and the resultant data were displayed as Fraser (1969) map (Figs. 5 and 6). Twelve profiles of these data (L100, L200,..., L1300) were selected for detailed interpretation and modelling (Fig. 7). The data were acquired at 10 m intervals and subsequently, data were first smoothed with 5-point averaging filter.

VLF anomalies are very sensitive to conductivity variations across strike, even small scale variations can be resolved to some extent, but without doubt VLF data are best in resolving lateral boundaries where the conductivity contrasts are strongest. The resultant data revealed that El-Sela shear zone conductive structures have a sufficiently considerable length along its strike so that it can be detected clearly. The filtered very low frequency electromagnetic (VLF-EM) map of the used frequency (17.1 kHz) indicates that the shear zone is distinguished with a strong conductivity (Fig. 5). This strong conductivity has been separated into parts of high amplitudes, resulting in an obvious exploration target. This zone is located on a broader discrete area, extending over a distance of about 1400 m and subjected to NNW–SSE displacements due to the parallel system of NNW–SSE trending left-lateral strike-slip faults.

The northern contact between the granite and Wadi sediments, showing a positive peak, is seen to have a shallow ascent. It is elongated in an ENE–WSW trend, and refers to the existence of conductive materials. This suggests that the contact is structurally controlled. Nevertheless, the granites are characterized by the presence of weakly conductive zones

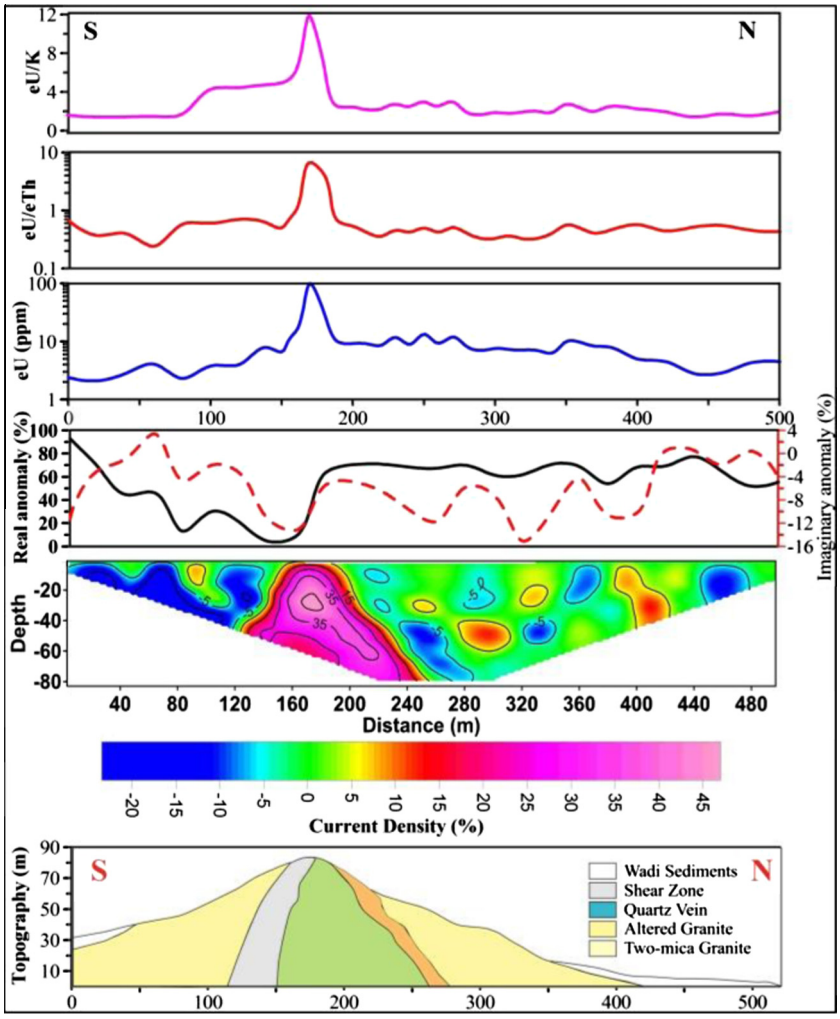

Figure 11 L400, VLF pseudo-sections, eU, eU/eTh, eU/K profiles and interpreted models of El-Sela Shear zone.

that generally follow the NW–SE and E–W trending faults. Meanwhile, the negative VLF-EM anomalies, located to the south of the shear zone, are due to highly resistive materials of quartz veins which dip steeply toward the south.

5. Interpreted structural lineaments

The interpreted structural lineaments, as deduced from the VLF-EM map (Fig. 6), have been employed to locate faulting, shearing and fracturing. Such lineaments can serve as potential hosts for a variety of minerals and indirectly guide exploration for the epigenetic, stress-related mineralization in the surrounding rocks. The structure interpretation of the VLF survey data clearly indicates the presence of the NNW–SSE, NW–SE, and ENE–WSW trending faults of strong conductive zone. Most of the NNW–SSE faults cause sudden change in the image spacing over an appreciable distance which suggests a discontinuity in depth due to these left lateral strike slip faults. Some of the NNW–SSE trends are interpreted as normal faults. The ENE–WSW trends are mostly associated with the main conductive shear zone in the study area. The NW–SE and NNW–SSE interpreted lineaments may be related to the conductive fractures and some strike slip faults. The ENE–WSW trending set of faults is older than the NNW–SSE trending set where the latter dissect and displace the former.

6. Results of VLF pseudo-sections, eU profiles and interpreted models

VLF pseudo-sections are fast and accurate in depicting the subsurfaces structure and widely used for VLF data interpretation. We have used this imaging technique to produce apparent current density cross-sections in the present study. Twelve profiles, namely, L100, L200, up to L1300, covering the studied area with intervals of around 100 m and profile length ranging from 250 m to 520 m were accomplished (Fig. 7). For the interpretation of the subsurface geometry, apparent current density cross-sections with depths were made using the acquired VLF data along all the profiles using Karous and Hjelt (1983). These apparent current density cross-sections are presented in Figs. 7–19 below the real and imaginary anomaly plots obtained from the VLF data acquired in the field. Results for surface gamma ray spectrometric measurements of eU, eU/eTh and eU/K are

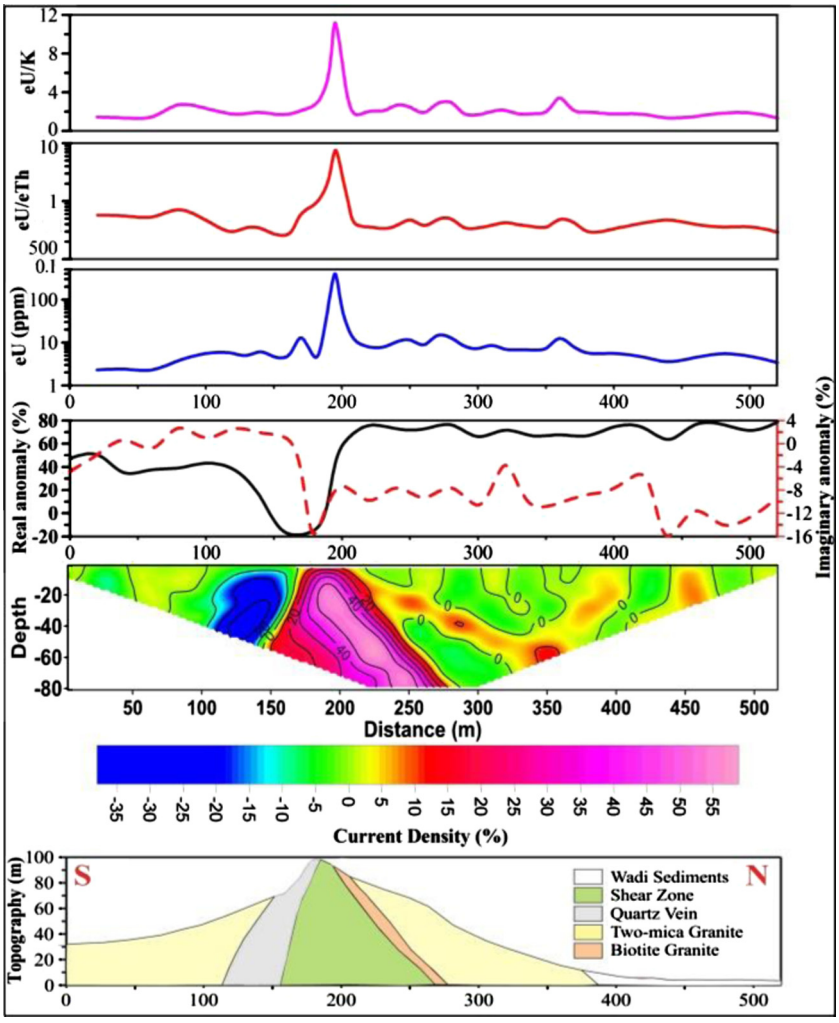

Figure 12 L500, VLF pseudo-sections, eU, eU/eTh, eU/K profiles and interpreted models of El-Sela Shear zone.

also shown as line plots along with VLF anomaly for every individual profile (Figs. 8–19). El-Sela shear zone is characterized by strong variation in the electrical conductivity.

This is typically due to alteration of the sheared rocks to mineralized clays causing an increase in the conductivities, whereas the adjacent granites and silica show low conductivity (Fig. 7). This is best developed along the central parts of the study area, where shearing and alteration show significantly higher conductivity values. The positive registered anomaly over the shear zone shows a gentle dip to the north and a steep dip to the south (Fig. 7).

6.1. Profile 1 (L100)

This profile, L100 (Figs. 7 and 8) is 100 m farther to the east of the first surveying profile of the study area. The real and imaginary anomaly plots indicate the presence of a high conductive anomaly at the south of the profile and multiple small conductive bodies along this profile (Fig. 8). Apparent current density cross-section also depicts the same result, showing the presence of high conductive body occurring near to the surface between stations 40 m and 100 m which suggests vertical structures to the south and gentle dip of about 45°, to the north as well as three limited and shallow, almost dipping to the north conductors between stations 140 m and 200 m, 280 m and 330 m, and 340 m and 400 m. Similarly, the radioactivity along this profile is higher than the background throughout the profile, with a peak between 40 m and 100 m. The peak values of eU, eU/eTh and eU/K at this station are 35 ppm, 4.5 and 17 respectively (Fig. 8).

6.2. Profile 2 (L200)

This profile, L200 (Fig. 7) is 100 m east of the profile L100. The real and imaginary anomaly plots indicate the presence of one strong anomaly located at the surface between stations 80 and 110 m and extend to depth of 80 m to become between stations 50 m and 140 m as shown in the apparent current density cross-section and in the interpreted lithological cross section (Fig. 9). Another two weak conductive bodies along this profile with vertical structures occur near to the surface

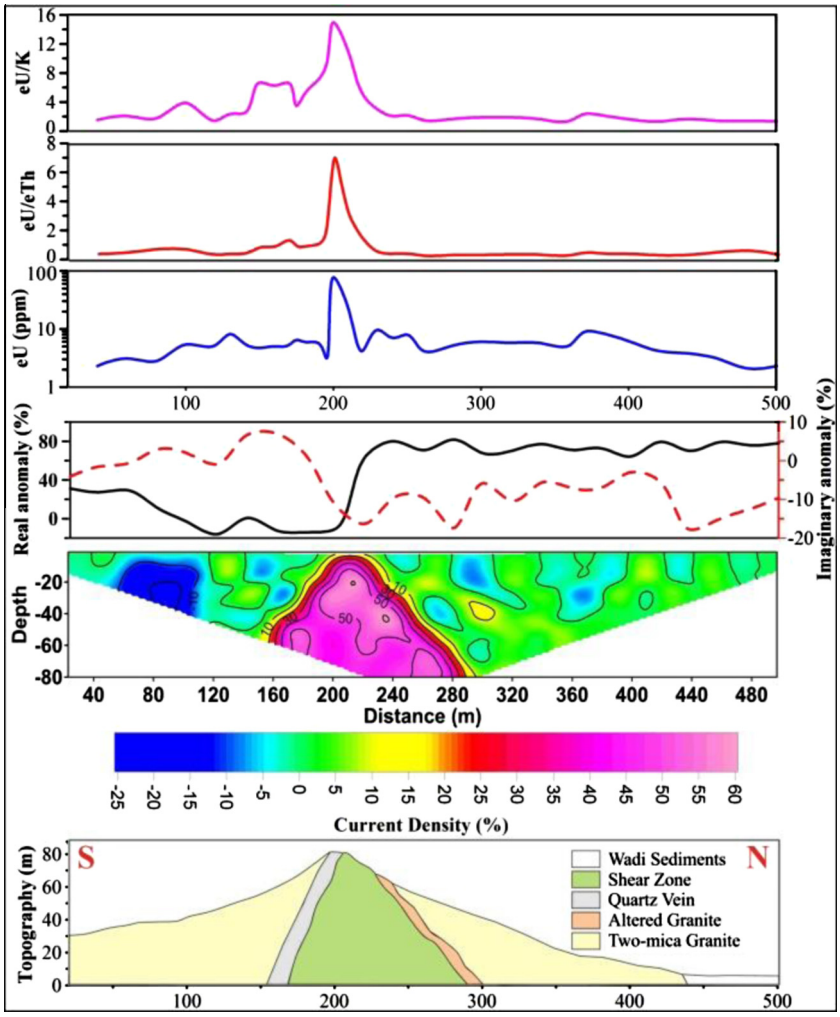

Figure 13 L600, VLF pseudo-sections, eU, eU/eTh, eU/K profiles and interpreted models of El-Sela Shear zone.

between stations 340 m and 380 m, and 430 m and 470 m. The uranium concentration (eU) and their ratios (eU/eTh and eU/K) along this profile depict a higher anomaly associated with the shear zone, located between stations 80 m and 130 m with values of 50 ppm, 2.5 and 9 respectively (Fig. 9). It correctly indicates a more conductive material on the southern side of this profile.

6.3. Profile 3 (L300)

Profile L300 lies 100 m east of profile L200 (Fig. 7). Here, also, the VLF anomaly curves indicate three conductive features, two are shallow and the third is buried. Apparent current density cross-section shows the presence of one high conducting and two low conducting structures between stations 100 m and 250 m, 280 m and 330 m, and 410 m and 470 m, respectively (Fig. 10). The conductor at the southern part of the profile (between stations 100 m and 250 m) is more conductive and wider among the three. Uranium content is observed to be highest above this conductor, with peak value of being 70 ppm at station 175 m. The eU/eTh and eU/K ratios are reaching 7 and 12 respectively.

6.4. Profile 4 (L400)

It lies 100 m east of profile L300 (Fig. 7). The VLF anomaly curves show four conductive features, all are shallow except one. Apparent current density cross-section indicates the presence of three low conducting structures between stations 220 m and 310 m, 310 m and 340 m, and 380 m and 430 m, respectively. Meanwhile, the strong conductor of high anomaly coincides with El-Sela shear zone that lies between stations 120 m and 250 m. This good conductor is steeply dipping to the south and gently to the north, so, it becomes wider at depth 80 m (Fig. 11). It is also well discriminated by its association with high uranium anomaly. The values of its eU, eU/eTh and eU/K are 100 ppm, 8 and 12 respectively, located at station 170 m (Fig. 11).

6.5. Profile 5 (L500)

This profile is 100 m away toward east of profile L400 (Fig. 7). VLF anomaly curves suggest the presence of a single conductor around station 200 m (Fig. 12). The slope of the anomaly curves indicates a thick inclined structure. Apparent current

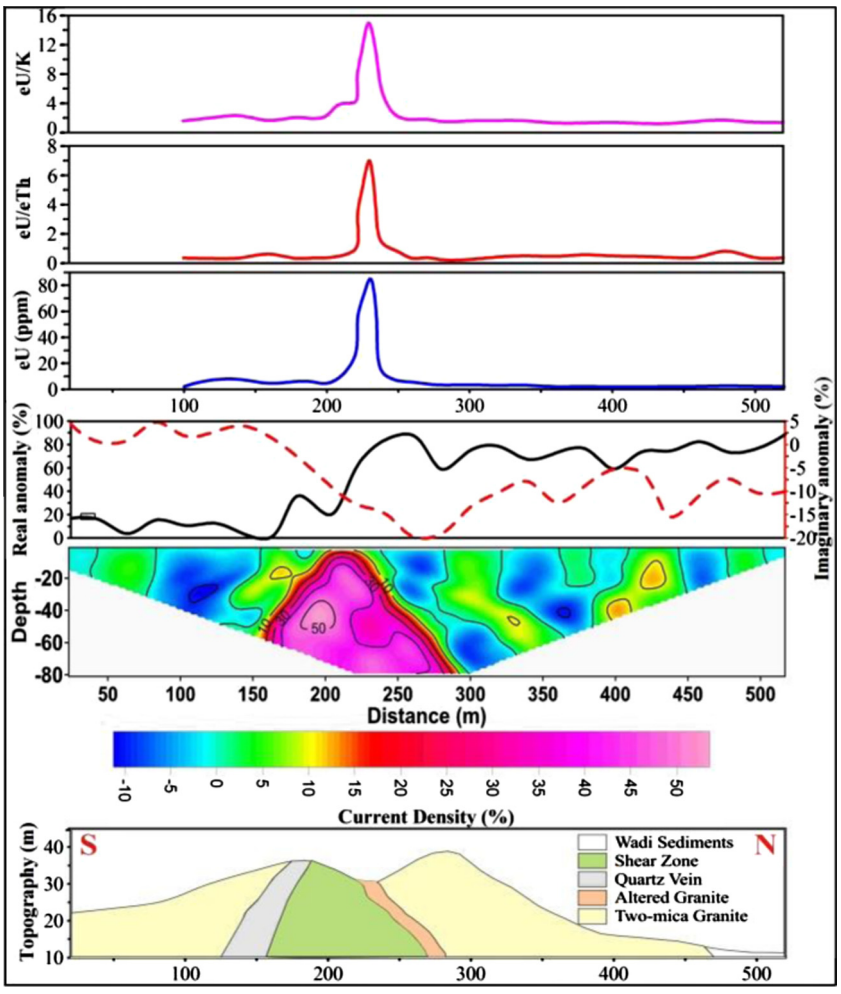

Figure 14 L700, VLF pseudo-sections, eU, eU/eTh, eU/K profiles and interpreted models of El-Sela Shear zone.

density cross-section confirms the presence of inclined conductive structure between stations 150 m and 270 m (Fig. 12). Radiometric data are observed to be almost equal to the background levels all along the profile with a sudden jump in value to 430 ppm of eU, 9 of eU/eTh ratio and 11 of eU/K ratio at station 200 m (Fig. 12).

6.6. *Profile 6 (L600)*

This profile is located at 100 m away from the profile L500 toward the east (Fig. 7). The input and quadrature VLF anomaly curves indicate the presence of one promising conductive anomaly between stations 140 m and 280 m (Fig. 13). The apparent current density cross-section and interpreted lithologic section show that the shape of the conductive body dip steeply to the south controlled with the barrier of quartz vein and dip gently to the north due to the altered granites. Accordingly, the width of that conductive body increases from 30 m near the surface to 140 m at depth of 80 m (Fig. 13).

Uranium concentration shows high radioactivity anomaly in the southern side of the profile compared to the northern side, with peak values 90 ppm, 7 and 14 respectively of eU, eU/eTh and eU/K found above the station 200 m (Fig. 13).

6.7. *Profile 7 (L700)*

This profile is located at the middle of the study area 100 m away from the profile L600 toward the east (Fig. 7). Both input and quadrature VLF curves depict the existence of two small buried conductive features around stations 330 m and 430 m (Fig. 14). Meanwhile, a big conductive body with width of about 50 m near the surface that increases gradually with depth reaching about 170 m at depth 80 m. The current density of this big body reaches to 57% indicating a highly conductive source as shown in the apparent current density cross-section (Fig. 14). Radiometric data show high radioactivity in the southern side of the profile compared to the northern side, with anomalies 85 ppm, 7 and 15 respectively of eU, eU/eTh and eU/K found above station 230 m (Fig. 14).

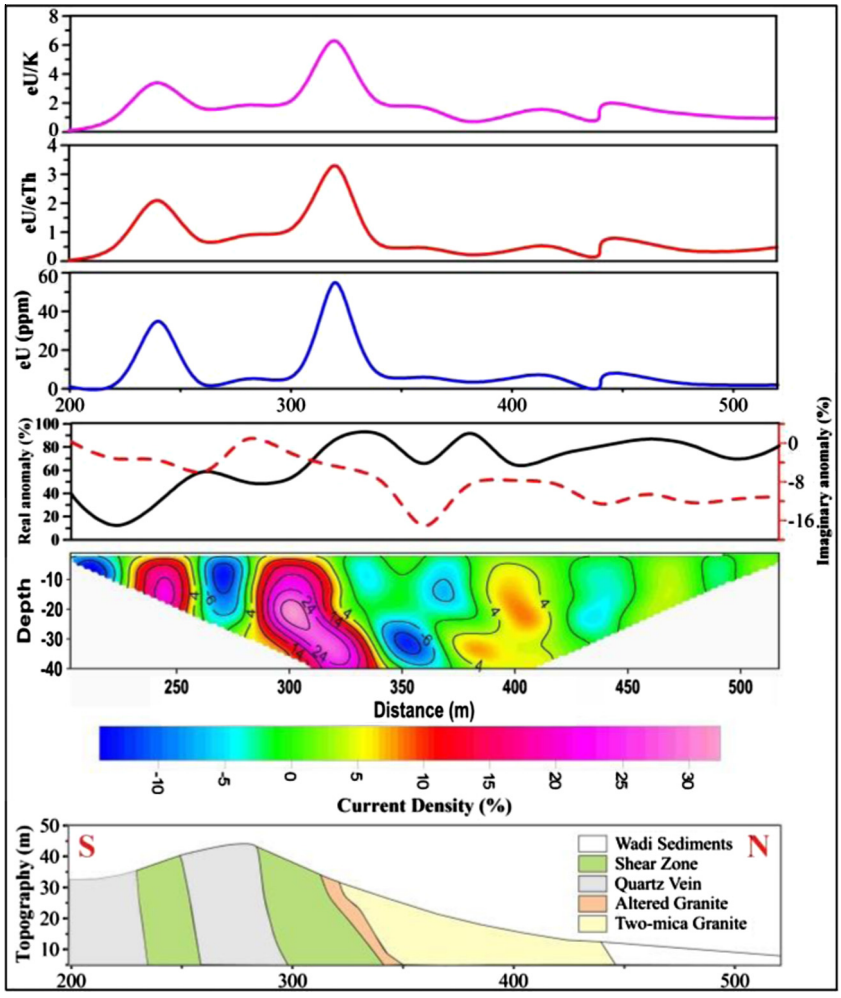

Figure 15 L800, VLF pseudo-sections, eU, eU/eTh, eU/K profiles and interpreted models of El-Sela Shear zone.

6.8. Profile 8 (L800)

This profile has length of 320 m, which less than the former profiles by about 200 m, (Fig. 7). The quadrature generally shows inverse correlation with the inphase profiles (Fig. 15). In both traces, the rapid fluctuations are consistent with a small skin depth and thus conductive surficial material over the granitic rocks. The strong apparent conductivity anomaly, observed over the shear zone, is caused by altered shear zone resulting high peaks in both inphase and quadrature profiles, with diverse polarity. However, the somewhat weak apparent conductivity anomalies located in the northeastern part of the study area correspond to other alterations in the granite and the northward displaced parts of the shear zone due to the left lateral strike slip faults. Whereas, radiometric data suggest two separated anomalies, one of them lies at station 240 m with values of 37 ppm eU, 2.3 eU/eTh ratio and 3.6 eU/K ratio, the second anomaly is located at station 322 m and slightly higher than the first one with values 55 ppm eU, 3.5 eU/eTh ratio and 6.5 eU/K ratio (Fig. 15).

6.9. Profile 9 (L900)

It has also 320 m length, and lies at 100 m east of L800 (Fig. 7), and the VLF anomaly curves indicate a single wide conductive feature lying all over the profile, with centre at 335 m (Fig. 16). Apparent current density cross-section also shows a much wider conductive feature lying between 290 m and 380 m, ranging in current density values from 7% to 35% (Fig. 16). This shows the same conducting level as profile L800 but lower than those in the central and eastern parts of the studied area. Radiometric data on the other hand suggest high uranium content, above the background level, only between stations 320 m and 380 m with values 50 ppm eU, 4.6 eU/eTh ratio and 11 eU/K ratio (Fig. 16).

6.10. Profile 10 (L1100)

It lies about 200 m east of profile L900, and VLF anomaly curves indicate the presence of one inclined conductor to the north direction (Figs. 7 and 17). Current density cross-section also shows high conductive feature between stations

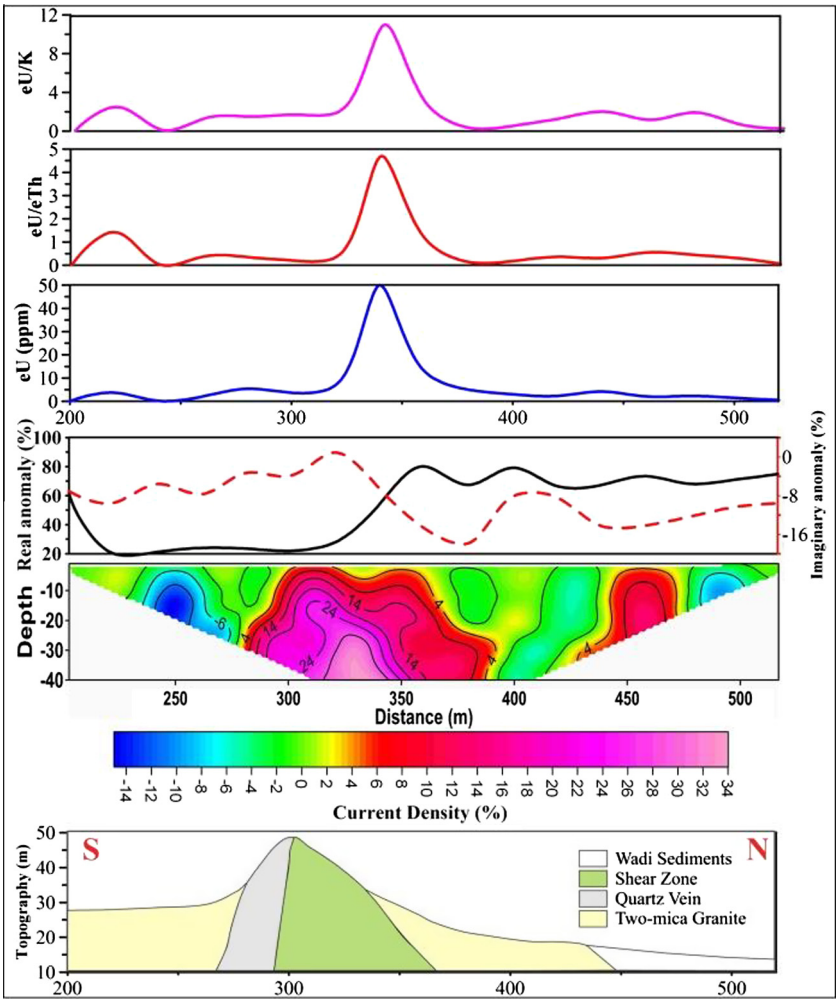

Figure 16 L900, VLF pseudo-sections, eU, eU/eTh, eU/K profiles and interpreted models of El-Sela Shear zone.

340 m and 400 m (Fig. 17). The current density reaches 30% indicating relatively low conductivity as compared to that of the eastern profiles (Fig. 17). High uranium concentration coincides with the conductive body reaching 120 ppm. The eU/eTh and eU/K ratios peaks up to 8 and 22 respectively, indicate the presence of high uranium content compared to low potassium and thorium concentrations.

6.11. Profile 11 (L1200)

This profile is about 100 m east of profile L1100 (Fig. 7). VLF anomaly curves indicate the presence of two conductors dipping to the south. Apparent current density pseudosection shows branching of the conductive body into two conductive features between stations 310 m and 3450 m and 410 m and 460 m (Fig. 18). The conductivity of these two separated bodies is less as compared to that of those bodies located at the western side of about 17% (Fig. 18). These relatively low conductivity anomalies, located in the western part of the study area, are caused by tension faults in the E–W direction followed by N–S sinistral strike-slip faults which displaced the parts of the shear zone. The two conductive bodies are associated also with high uranium anomalies reaching 60 ppm (eU), 6.5 (eU/eTh) and 16 (eU/K) for the south body and 80 ppm (eU), 7.3 (eU/eTh) and 19 (eU/K) for the northern one (Fig. 18).

6.12. Profile 12 (L1300)

It lies 100 m east of profile L1200 (Fig. 7), and VLF anomaly curves indicate the presence of two vertical conductors. The VLF-EM curves show marked changes in polarity along the shear zone. This reveals anomalies around the same location, with the shapes and consistent with a conductive target. Current density section traces the two conductive features between stations 330 m and 380 m and 415 m and 460 m (Fig. 19). The southern one is highly conductive as compared to the northern one.

The uranium curves indicate that the conductivity is essentially due to the shear zone mineralization, with no contribution from the adjacent granite. There are two peak regions of uranium and their ratios around stations 350 m and

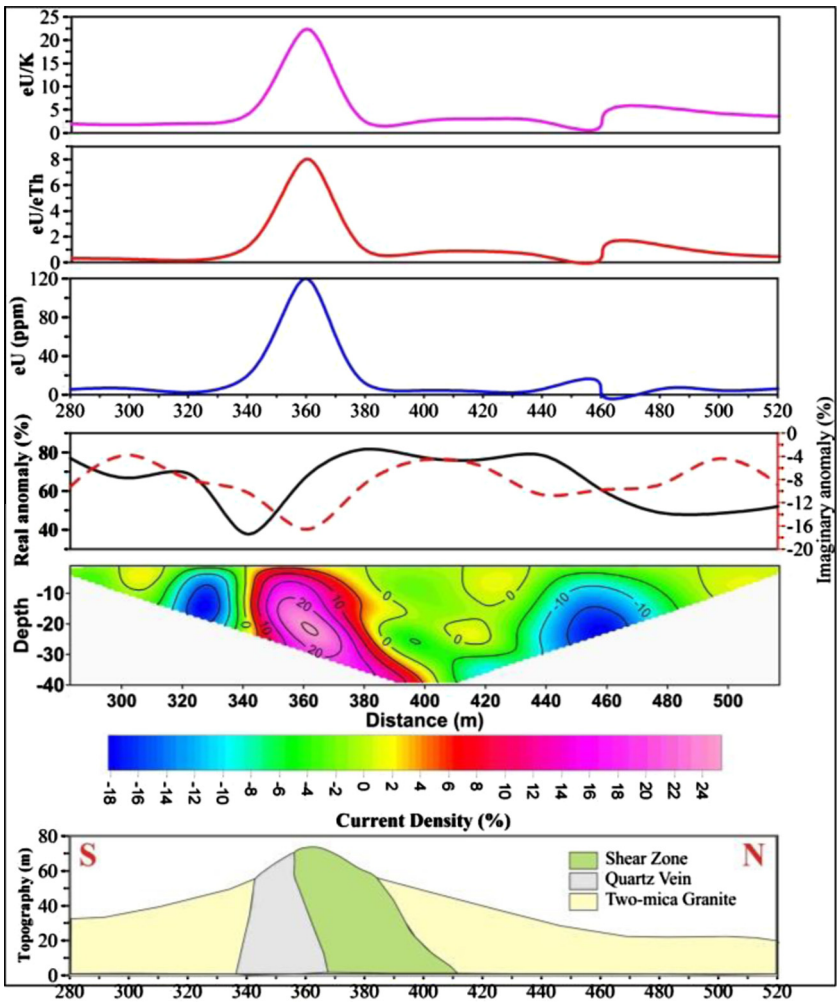

Figure 17 L1100, VLF pseudo-sections, eU, eU/eTh, eU/K profiles and interpreted models of El-Sela Shear zone.

440 m (Fig. 19). These wide VLF-EM anomalies are typical of good conductors, which are in agreement with the eU, eU/eTh and eU/K values of 65 ppm, 4.2, 16.3 for the first body and 40 ppm, 3, 10 for the second conductive body.

7. Discussion

In the present study, seventy profiles data were filtered using Fraser filter and the resultant data were constructed as map (Fig. 5). Twelve profiles were chosen cut across the El-Sela shear zone using Karous–Hjelt filter for construct pseudo-sections (Figs. 7–19) to investigate the uranium mineralization by applying VLF-EM and radiometric methods together. Results show the presence of a promising conductive zone and multiple isolated conductive features in the study area. The promising conductive zone is associated with the El-Sela shear zone filled with fluids, hydrothermal alterations, uranium mineralization and shearing clay, whereas, the separated small conductive features appearing in the profiles could indicate the presence of fractures filled with mineralization (Figs. 7–19).

The high conductive features are traced continuously well in all the profiles, showing a regular parallel trend except in profiles L1200 and L1300 in the eastern part of the study area where two conductive parts separated by high resistive zone are encountered. This implies that the highly conductive shear zone at the eastern part of the study area is divided into two parts separated by granite and quartz rocks. This offset of the current density anomaly could be due to strike slip fault, where the observed anomalies appear vertical in the current density profile and the offset or movement is lateral along the strike of the fault. This happens in case of strike-slip fault; hence, it appears to be the better reason for such lateral shift of the mineralized body. This can be further substantiated by successive structural mapping of the area.

The separation between the conductive bodies is not uniform along all the profiles. This further suggests that these mineralized bodies have small strike length and lenticular shape. This result together with the geology of the area indicates that the mode of mineralization is hydrothermal alteration (Ibrahim et al., 2009 and Gaafar et al., 2014, 2015).

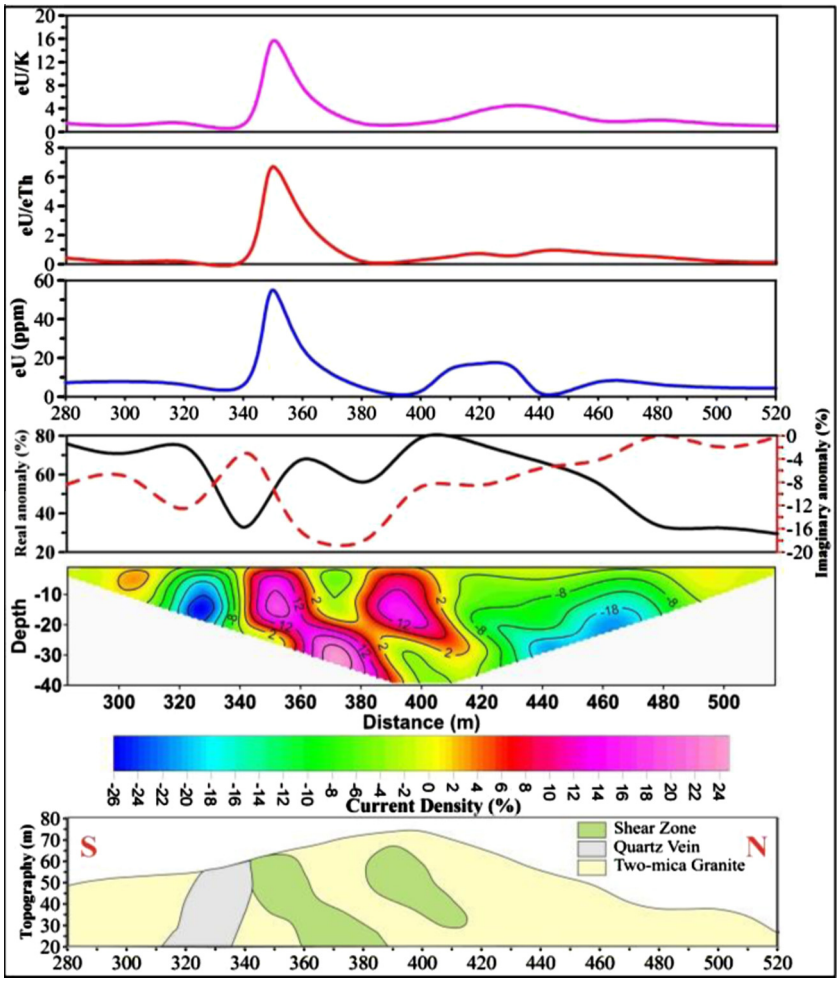

Figure 18 L1200, VLF pseudo-sections, eU, eU/eTh, eU/K profiles and interpreted models of El-Sela Shear zone.

Radiometric measurements indicate higher radiations along the profiles than the average or background radiations observed in the area. The peak or elevated eU as well as their ratios eU/K and eU/eTh indicate the presence of uranium mineralization. Surface gamma-ray activity superimposed over geological map of the area of study clearly depicts the coincidence of conductive zones and high radioactivity zones (Figs. 2–5 and 7). This coincidence confirms the existence of high alteration zones in this area. These zones may be enriched with uranium mineralization as they are also correlating with the radioactive minerals from the borehole data identified by Gaafar et al. (2014). All these identified mineralized zones are almost parallel and have a collective strike oriented along ENE direction which is in agreement with the strike of El-Sela shear zone. Here, El-Sela Shear Zone is associated with conspicuous, coincident, elongated positive conductivity anomalies. The advantage of this integrated approach is their rapidness and cost-effectiveness and, hence, it can be used as a quick mapping and subsurface imaging tool for scanning structures associated with uranium mineralization.

The association of uranium and conductivity anomalies for El-Sela shear zone would be sufficient indication of the most promising uranium vein-type target. It is representing a good trap for U-rich fluids and/or U-mineralization which is a great incentive for drilling.

8. Conclusions

VLF-EM and radiometric methods were applied together in the study area to utilize their integrated results for the uranium exploration. Results indicate good correlation between VLF data and radiometric data. This is because these radiometric signals are associated with shallow uranium mineralization which is associated with altered minerals that give conductivity contrast with the neighbouring rocks. Coincidence of high radioactivity over the conductive zones observed in the area confirms the presence of uranium mineralization. Thus, the study also suggests that these two methods can be integrated to explore uranium mineralization effectively at low cost with the advantage of being quick compared to other routine methods used for such purpose. The study also reveals the presence of a system of left lateral strike slip faults elongated in the NNW direction, proving the ability and advantage of this integrated approach in detecting such planner structures and

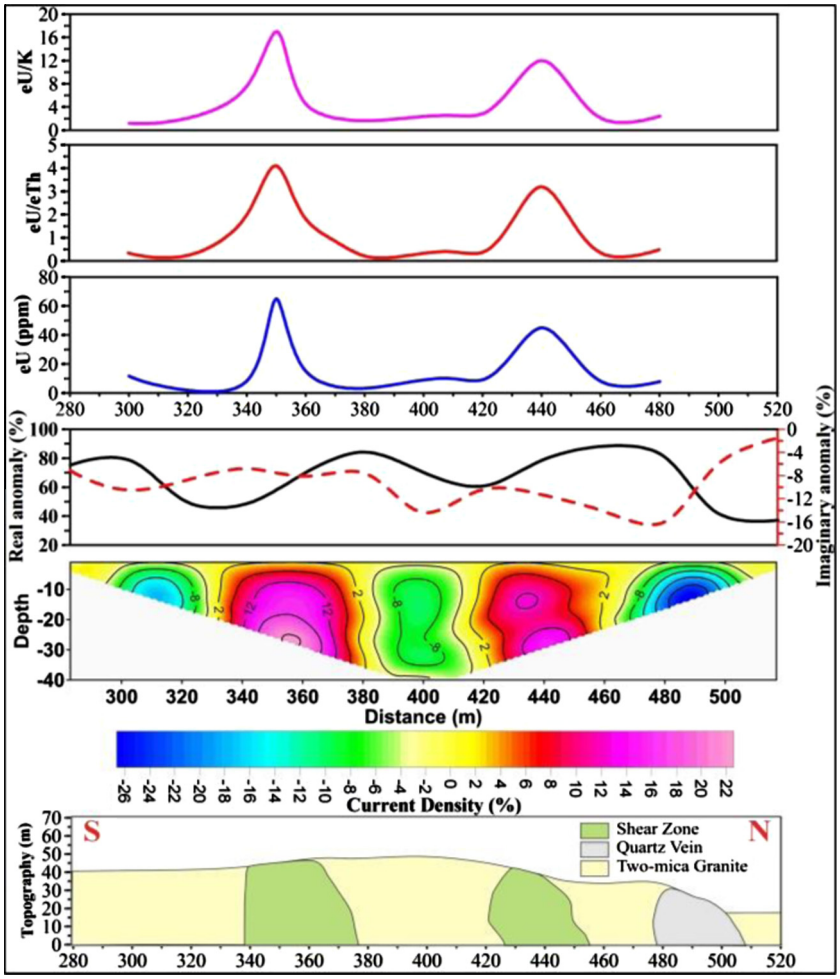

Figure 19 L1300, VLF pseudo-sections, eU, eU/eTh, eU/K profiles and interpreted models of El-Sela Shear zone.

correlating the lithology both vertically and laterally. Since, these methods are quick and cost effective, they can be utilized to search for shallow uranium mineralization along the uranium vein type and similar regions. The combined interpretation of the geological and the VLF-EM results indicates that the shear zone has a large thickness especially in the central part of the studied area which decreases gradually to the east and west directions. The obtained models by the pseudo-sections of the VLF-EM data strongly suggest that the shear zone of the survey area takes a shape of a cone with the top thickness of 50 m at the surface and a base width of about 150 m at depth of 80 m.

References

Ali, K.G., 2011. Structural control of El Sela granites and associated uranium deposits, Southern Eastern Desert, Egypt. Arab J. Geosci. http://dx.doi.org/10.1007/s12517-011-0489-y.

Becken, M., Pedersen, L.B., 2003. Transformation of VLF anomaly maps into apparent resistivity and phase. Geophysics 68, 497–505.

Benson, A.K., Payne, K.L., Stubben, M.A., 1997. Mapping groundwater contamination using dc resistivity and VLF geophysical method — a case study. Geophysics 62 (1), 80–86.

Charbonneau, B.W., Ford, K.L., 1979. Discovery of two uranium occurrences in Paleozoic sedimentary rocks at South March, Ontario and South Maitland, Nova Scotia. J. Canad. Soc. Explor. Geophys. 15 (1), 54–76.

Duval, J.S., 1983. Composite color images of aerial gamma-ray spectrometric data. Geophysics 48, 722–735.

Fischer, G., Le Quang, B.V., Müller, I., 1983. VLF ground surveys, a powerful tool for the study of shallow two-dimensional structures. Geophys. Prospect. 31 (6), 977–991.

Fraser, D.C., 1969. Contouring of VLF-EM data. Geophysics 34, 958–967.

Gaafar, I.M., 2012. Geophysical signature of the vein-type uranium mineralization of Wadi Eishimbai, Southern Eastern Desert, Egypt. Arab. J. Geosci. 5, 1185–1197.

Gaafar, I.M., Ghazala, H.H., Ibrahim, T.M., Ammar, S.E., 2006. Application of Ground Magnetic Survey for Defining the Subsurface Structural Pattern of West Abu Ramad Shear Zone, Southern Eastern Desert, Egypt. In: the 8th SEGJ International Symposium – Imaging and Interpretation – Kyoto, Japan, 2006, pp. 487–492.

Gaafar, I.M., Cuney, M., Gawad, A., 2014. Mineral chemistry of two-mica granite rare metals: impact of geophysics on the distribution of uranium mineralization at El-Sela Shear Zone, Egypt. Open J. Geol. 4, 137–160.

Gaafar, I.M., Aboelkheir, H., Bayoumi, M., 2015. Integration of Gamma-Ray Spectrometric and Aster Data for Uranium

Exploration in Qash Amer-El-Sela Area, Southeastern Desert, Egypt. Nuclear Sciences Scientific Journal (in press).

Ibrahim, T.M., Abdel Ghany, M.S., Ali, K.G., Gaafar, I.M., 2009. Characterization of new surfacial uranium deposit in El-Sela Area, South Eastern Desert, Egypt. Annals Geol. Surv. Egypt 31, 405–415.

Karous, M., Hjelt, S.E., 1983. Linear filtering of VLF dip-angle measurements. Geophys. Prospect. 31 (5), 782–794.

Legault, J.M., Carriere, D., Petrie, L., 2008. Synthetic model testing and distributed acquisition dc resistivity results over an unconformity uranium target from the Athabasca Basin, northern Saskatchewan. Leading Edge 27 (1), 46–51.

McNeill, J.D., Labson, V.F., 1991. Geological mapping using VLF radio fields. In: Nabighian, M.N. (Ed.), Electromagnetic Methods in Applied Geophysics, V2, Application, Part B. SEG, Tulsa, pp. 521–640.

Nimeck, G., Koch, R., 2008a. A progressive geophysical exploration strategy at the Shea Creek uranium deposit. Leading Edge 27 (1), 52–63.

Nimeck, G., Koch, R., 2008b. A progressive geophysical exploration strategy at the Shea Creek uranium deposit. Leading Edge, 52–63.

Sharma, S.P., Baranwal, V.C., 2005. Delineation of groundwater-bearing fracture zones in a hard rock area integrating very low frequency electromagnetic and resistivity data. J. Appl. Geophys. 57, 155–166.

Smith, R.S., Annan, A.P., McGowan, P.D., 2001. A comparison of data from airborne, semi-airborne, and ground electromagnetic systems. Geophysics 66, 1379–1385.

Tabbagh, A., Benderitter, Y., Andrieux, P., Decriaud, J.P., Guerin, R., 1991. VLF resistivity mapping and verticalisation of the electric field. Geophys. Prospect. 39, 1083–1097.

Tuncer, V., Unsworth, M.J., Siripunvaraporn, W., Craven, J.A., 2006. Exploration for unconformity-type uranium deposits with audio-magnetotelluric data: a case study from the McArthur River mine, Saskatchewan, Canada. Geophysics 71 (6), B201–B209.